

Concepts and Performance Results on the Combination of Different Integrity Methods Using UAIM and GNSS without SA

Erwin Loehnert, Robert Wolf, Juergen Pielmeier, Wolfgang Werner
IfEN Gesellschaft für Satellitennavigation mbH (IfEN GmbH), D-85579 Neubiberg, Germany

Theodor Zink
Institute of Geodesy and Navigation (IfEN), University FAF Munich, D-85577 Neubiberg, Germany

BIOGRAPHIES

Erwin Löhnert received a diploma in Aerospace Engineering in 1993 from the Munich University of Technology. In 1994 he joined the Institute of Geodesy and Navigation (IfEN) of the University FAF Munich as a Research Associate, working mainly for aerogravimetry and GPS/INS integration. Since 2000 he is a Project Manager at IfEN Gesellschaft für Satellitennavigation mbH (IfEN GmbH) working for integrity determination.

Robert Wolf received a diploma in Aeronautical Engineering in 1995. He worked as a research associate at IfEN. His main activities were in the field of GPS/INS hybridisation, Kalman filtering and orbit determination. Since 1999 he is working for IfEN GmbH, where he is involved in the integrity algorithm development for the Independent Check Set of the EGNOS system.

Jürgen Pielmeier studied Aerospace Engineering at the University of Technology in Berlin. He worked as a research associate at IfEN and was mainly concerned with research in the field of GPS RAIM Availability. Since 1999 he is Managing Director of IfEN GmbH.

Wolfgang Werner received in 1994 a diploma in Computer Science from the University of Technology in Munich. He worked as a Research Associate at IfEN in the field of high-precision DGPS, ambiguity resolution and APL (airport pseudolite) research. In 2000 he received his PhD from the University FAF Munich. Since 1999 he is Technical Director of IfEN GmbH.

Theodor Zink is Research Associate at IfEN. In 1995 he received a diploma in Electrical Engineering from the University of Erlangen-Nuremberg. He is currently concerned with research in the fields of GPS/GLONASS RAIM as well as of EGNOS/GNSS integrity.

ABSTRACT

A second generation GNSS has to overcome especially one basic deficiency of present satellite navigation systems as the U.S. GPS and the Russian GLONASS, i.e. the lack of integrity in the Signal-In-Space (SIS). Thus, the European contribution to GNSS-2 (Galileo) requires that the SIS shall provide integrity for Category I precision approach and landing.

The integrity of a system refers to the assurance that all functions of this system perform within the operational limits where the integrity risk is the probability of undetected failures resulting in the loss of specified accuracy. Analyses of appropriate integrity monitoring techniques for a GNSS-2 must be performed in order to demonstrate whether or not this performance requirement can be met by the proposed GNSS-2 architectures.

The paper discusses basic integrity monitoring concepts as Receiver Autonomous Integrity Monitoring (RAIM) like methods for the Galileo users and the contribution of ground-based integrity monitoring as well as results of an adapted RAIM algorithm availability simulation. Because RAIM alone is very likely insufficient to fulfil all requirements necessary for a broad spectrum of users (e.g. civil aviation) several techniques have been proposed for combining RAIM with external systems (e.g. LORAN-C, GIC) or independent sensors like inertial sensors, barometer etc. Those techniques are commonly known as User Autonomous Integrity Monitoring (UAIM). Firstly, an approach for generic RAIM algorithms to be used for GNSS without Selective Availability SA (GPS since 2nd May 2000, Galileo) is outlined. Then, basic concepts and techniques for user integrity monitoring using RAIM and hybridisation are presented. Finally, a first performance assessment of the combination of different UAIM techniques and concluding remarks will be given.

INTRODUCTION

The general purpose of integrity monitoring is the protection of a service provided by a system against errors, which exceed a specified bound. This protection of a system service can be achieved by several methods, where redundant information is used by either a single independent autonomous subsystem or by a combination of independent autonomous subsystems in order to check the correctness of this service and/or the total system is monitored by an external independent monitoring system.

Independent autonomous integrity monitoring performed by a Galileo user receiver aims at the protection of the user navigation solution against position errors exceeding the alarm limit. For this reason, the integrity monitor of a user receiver must provide a timely warning when a failure exists (i.e. when a position error exceeds the alarm limit). In addition to this, if a user receiver utilizes additional information from the Ground Integrity Channel (GIC) of Galileo, from further navigation systems and/or from other sensors, then the integrity of the navigation solution, which is provided by this user receiver, increases.

The following discussion with regard to the navigation solution integrity monitoring by the user receiver gives a first preliminary qualitative assessment of the integrity monitoring level, which can be achieved at user level, as well as of the impact of the GIC on the integrity monitoring level. Moreover, the hybridisation of Galileo with other navigation systems and/or with further sensors is considered.

USER AUTONOMOUS INTEGRITY MONITORING BASICS

All measurements used by the user receiver for determining the navigation solution are also used by the integrity monitor of this user receiver in order to check the consistency of this navigation solution. In general, independent autonomous integrity monitoring performed by a Galileo user receiver is structured as follows:

- (i) **User integrity monitor availability check** (checks, if number of used measurements as well as relative geometry of the user receiver position and the satellite positions are sufficient for monitoring correctness of the navigation solution, which meets the user performance requirements)
- (ii) **Hypothesis test** (checks, if one of the measurements used is incorrect, assuming that the integrity monitor is available as well as only one of these measurements is incorrect at a time)

If the integrity monitor of a user receiver is not available, e.g. due to insufficient relative geometry, then the navigation solution consistency check (hypothesis test) cannot be performed and the user performance requirements cannot be met. In this case, the user has to use measurements from other navigation systems or sensors in order to determine a correct navigation solution, which meets the user performance requirements. If the availability check is passed, then a hypothesis test (i.e. the calculation of a test statistic and the subsequent comparison of this test statistic with the concerning threshold) may be performed by the integrity monitor in order to decide whether or not an incorrect measurement exists. If no incorrect measurement is detected (i.e. this test statistic is smaller than or equal to this threshold), then it is assumed that the navigation solution calculated by the user is a correct navigation solution, meeting the user performance requirements. Otherwise an incorrect measurement is detected (i.e. the test statistic is greater than the threshold) and the navigation solution computed by the user is assessed as incorrect. In this case, the user has to perform one of the following operations in order to obtain a correct navigation solution meeting the user performance requirements:

- (i) Determination of a correct navigation solution, by using only measurements from other navigation systems or sensors
- (ii) Isolation, i.e. identification, and/or exclusion of the incorrect measurement from the navigation solution

It must be noted that fault isolation/exclusion is only required for primary means of navigation as well as for sole means of navigation. Moreover, the relative geometry of the user receiver position and the satellite positions is not always sufficient for the fault isolation/exclusion purpose. Therefore, the user cannot compute a correct navigation solution meeting the user performance requirements when an incorrect measurement is detected and when fault isolation/exclusion cannot be performed as well as when no other measurements than those used by the user for the determination of the navigation solution, which is assessed as incorrect, are available.

ADAPTED RAIM ALGORITHM

Under the existing methods for integrity monitoring at user level, RAIM like techniques are very suitable for checking the correctness of the navigation solution provided by the user receiver. Assuming that the least squares adjustment is used by the user receiver in order to determine the navigation solution, then the RAIM method proposed by Brenner [1] can be modified in order to obtain an adapted RAIM algorithm, which can be used by

the integrity monitor of this user receiver and which is also applicable when a GNSS-2 (Galileo) is hybridised with other navigation systems and/or with further sensors. This adapted RAIM algorithm is the basis for the following analyses of the navigation solution integrity monitoring performed by the user receiver and is denoted as the parity method with aligned coordinate systems.

Mathematical Model

The mathematical model, which is used by the adapted RAIM algorithm, bases on the assumption that at a given point in time n measurements are available at the user receiver. It is additionally assumed that $n > m$ for fault detection as well as $n > m+1$ for fault detection and isolation/exclusion, where m is the number of unknowns. The unknowns are the three user receiver position coordinates and the user receiver clock offset with respect to the Galileo network time (i.e. the number of unknowns is equal to four when the user receiver uses only Galileo satellite measurements). Note that the hybridisation of Galileo with other navigation systems and/or with further sensors generally results in additional unknowns (e.g. user receiver clock offsets with respect to the network times of other navigation systems when Galileo is hybridised with further navigation systems). The linearisation of the non-linear functions, which belong to the n measurements, of the unknowns yields the relationships between these n measurements and the unknowns in the form of the following system of linear algebraic equations:

$$\mathbf{y}_M = \mathbf{G}_M \mathbf{x} + \boldsymbol{\varepsilon}_M \quad (1)$$

with

\mathbf{y}_M	$n \times 1$ residual vector
\mathbf{G}_M	$n \times m$ design matrix with $\text{rank}(\mathbf{G}_M) = m$
\mathbf{x}	$m \times 1$ vector of the deviations of the unknowns from the predicted values of the unknowns
$\boldsymbol{\varepsilon}_M$	$n \times 1$ error vector

The residual vector consists of the differences between the values of these nonlinear functions at the unknowns and the values of these nonlinear functions at the predicted values of the unknowns. Furthermore, the elements in each row of the design matrix are the first order partial derivatives of the corresponding nonlinear function at the predicted values of the unknowns. The first order partial derivatives, which are the elements of a row of the design matrix, are thereby obtained by Taylor series expansion of the corresponding nonlinear function yielding the linear algebraic equation, which belongs to this row of the design matrix. It must be noted that the first three components of \mathbf{x} are the three components of the user receiver position deviation from the predicted user receiver position. Moreover, the error vector is Gaussian with zero mean vector and with constant

positive definite covariance matrix \mathbf{R}_{cov} , i.e. $\boldsymbol{\varepsilon}_M \sim \mathbf{N}(\mathbf{0}, \mathbf{R}_{cov})$. The $n \times n$ matrix \mathbf{R}_{cov} is specified by $\mathbf{R}_{cov} = (\mathbf{W}^T \mathbf{W})^{-1}$ with the $n \times n$ diagonal matrix

$$\mathbf{W} = \text{diag}(\sigma_1^{-1}, \dots, \sigma_n^{-1}) \quad (2)$$

where σ_i is the standard deviation of the i th component of the error vector ($\sigma_i > 0 \forall i \in \{1, \dots, n\}$). If the i th component of the error vector belongs to a Galileo satellite measurement, then the variance σ_i^2 of this component of $\boldsymbol{\varepsilon}_M$ is specified as follows [5]:

$$\sigma_i^2 = \sigma_{SISA,i}^2 + \frac{\sigma_{UIVE,i}^2}{1 - \left(\frac{R_e \cos E_i}{R_e + h_I} \right)^2} + \sigma_{SNR,i}^2 + \frac{\sigma_{m45}^2}{\tan^2 E_i} + \frac{\sigma_{trv}^2}{\sin^2 E_i} \quad (3)$$

with

σ_i	Standard deviation of the i th component of $\boldsymbol{\varepsilon}_M$
$\sigma_{SISA,i}$	Standard deviation of the combined satellite ephemeris and clock error contribution
$\sigma_{UIVE,i}$	Standard deviation of the vertical ionospheric error contribution
R_e	Mean radius of the earth
E_i	Elevation angle of the satellite
h_I	Height of the maximum electron density
$\sigma_{SNR,i}$	Standard deviation of the user receiver noise contribution
σ_{m45}	Standard deviation of the multipath error contribution at 45 degrees
σ_{trv}	Standard deviation of the vertical tropospheric error contribution

Note that the standard deviation $\sigma_{SISA,i}$ of the combined satellite ephemeris and clock error contribution is determined by the Signal In Space Accuracy (SISA), which is provided by Galileo to the users, of the corresponding satellite since the SISA of a satellite is a $k \cdot \sigma$ bound of the corresponding measurement error component, which is caused by the combined ephemeris and clock error of this satellite (i.e. $\sigma_{SISA,i} = \text{SISA}_i/k$; $i = \text{satellite index}$). In addition to this, the standard deviation $\sigma_{UIVE,i}$ of the vertical ionospheric error contribution can be assumed to be very small, when a Galileo dual-frequency receiver is used for positioning.

Now, the substitutions $\mathbf{y} = \mathbf{W}\mathbf{y}_M$, $\mathbf{G} = \mathbf{W}\mathbf{G}_M$ and $\boldsymbol{\varepsilon} = \mathbf{W}\boldsymbol{\varepsilon}_M$ are used in order to obtain the following system of normalized linear algebraic equations:

$$\mathbf{y} = \mathbf{G}\mathbf{x} + \boldsymbol{\varepsilon} \quad (4)$$

where

\mathbf{y}	$n \times 1$ normalized residual vector
\mathbf{G}	$n \times m$ normalized design matrix
\mathbf{x}	$m \times 1$ vector of the deviations of the unknowns from the predicted values of the unknowns
$\boldsymbol{\varepsilon}$	$n \times 1$ normalized error vector

Furthermore, it is additionally assumed that no more than one of the n measurements is incorrect and that an incorrect measurement is represented by the corresponding component, which has a mean that is not equal to zero, of the normalized error vector.

Adapted RAIM Algorithm Availability

The availability of the integrity monitor of a user receiver must be checked in order to decide if the (user receiver) integrity monitoring meets the user performance requirements. The user integrity monitor availability check of the parity method with aligned coordinate systems bases on the QR decomposition $\mathbf{G} = \mathbf{Q}\mathbf{R}$ of \mathbf{G} where the $n \times n$ matrix \mathbf{Q} is an orthogonal matrix and the $n \times m$ matrix \mathbf{R} has zeros in row $m+1$ to n and an upper triangular $m \times m$ matrix \mathbf{R}_x in row 1 to m . Moreover, $\mathbf{Q} = (\mathbf{Q}_x^T, \mathbf{Q}_p^T)$ is partitioned into the $n \times m$ matrix \mathbf{Q}_x^T and the $n \times (n-m)$ matrix \mathbf{Q}_p^T . In addition to this, an orthogonal $(n-m) \times (n-m)$ matrix \mathbf{A}_k is chosen so that the first element of the k th column of the $(n-m) \times n$ matrix $\mathbf{P}_k = \mathbf{A}_k \mathbf{Q}_p$ is p_{1k} and all other elements of the k th column of \mathbf{P}_k are zero. The threshold can be determined by

$$d_T = F_{\text{CEF}}^{-1}(P_{fa}/2n), \quad (5)$$

using the complementary error function

$$F_{\text{CEF}}(t) = \frac{1}{\sqrt{2\pi}} \int_t^{\infty} e^{-y^2/2} dy \quad (6)$$

with

d_T	Threshold
$F_{\text{CEF}}^{-1}(t)$	Inverse of complementary error function
P_{fa}	False alarm probability
n	Number of measurements

The false alarm probability is thereby specified as follows:

$$P_{fa} = r_{fa} \cdot t_{CT} \quad (7)$$

where

P_{fa}	False alarm probability
r_{fa}	False alarm rate
t_{CT}	Correlation time of measurement errors

If the standard deviation of one of the measurement error components of the used sensors and navigation systems is significantly larger than the other standard deviations, then the correlation time t_{CT} of this measurement error component is used for the computation of the false alarm probability P_{fa} . Otherwise, if no significantly larger standard deviation exist, a set of large (including the largest) standard deviation exist, which lie in the same order of magnitude. From this set the largest correlation time t_{CT} is chosen to calculate false alarm probability P_{fa} . Thus, the Horizontal Protection Level (HPL) as well as the Vertical Protection Level (VPL) can be given as follows:

$$\text{HPL} = \text{Max}_{k=1, \dots, n} \left[\frac{d_T + F_{\text{CEF}}^{-1}(P_{md})}{|p_{1k}|} \cdot \sqrt{b_{1k}^2 + b_{2k}^2} \right] \quad (8)$$

$$\text{VPL} = \text{Max}_{k=1, \dots, n} \left[\frac{d_T + F_{\text{CEF}}^{-1}(P_{md})}{|p_{1k}|} \cdot |b_{3k}| \right] \quad (9)$$

where

d_T	Threshold
$F_{\text{CEF}}^{-1}(t)$	Inverse function of the complementary error function
P_{md}	Missed detection probability
p_{1k}	First element of k th column of \mathbf{P}_k
b_{1k}	First element of the k th column of the $m \times n$ matrix $\mathbf{B} = \mathbf{C}_L(\mathbf{G}^T \mathbf{G})^{-1} \mathbf{G}^T$
b_{2k}	Second element of the k th column of the $m \times n$ matrix $\mathbf{B} = \mathbf{C}_L(\mathbf{G}^T \mathbf{G})^{-1} \mathbf{G}^T$
b_{3k}	Third element of the k th column of the $m \times n$ matrix $\mathbf{B} = \mathbf{C}_L(\mathbf{G}^T \mathbf{G})^{-1} \mathbf{G}^T$
n	Number of measurements

The $m \times m$ matrix \mathbf{C}_L represents the linear transformation that transforms the three user receiver position deviation components of \mathbf{x} to the topocentric local Cartesian coordinate system with its axes along the local north, local east and local vertical down at the user receiver position whereas the remaining components of \mathbf{x} are not changed by this linear transformation.

The missed detection probability can be defined by

$$P_{md} = r_{md} \cdot t_{CT} \quad (10)$$

with

P_{md}	Missed detection probability
r_{md}	Missed detection rate
t_{CT}	Correlation time of the measurement errors

The adapted RAIM algorithm is available for horizontal navigation, if $\text{HPL} \leq \text{Horizontal Alarm Limit (HAL)}$ is fulfilled. The algorithm is available for vertical

navigation, if $VPL \leq$ Vertical Alarm Limit (VAL) is fulfilled.

Fault Detection Method

The fault detection algorithm of the parity method with aligned coordinate systems bases also on the matrices \mathbf{P}_k . If \mathbf{p}_k^T ($k = 1, \dots, n$) are the first rows of these matrices \mathbf{P}_k , then the test statistics are given as follows:

$$d_k = \mathbf{p}_k^T \mathbf{y} \quad (11)$$

This adapted RAIM algorithm decides that no incorrect measurement exists when $|d_k| \leq d_T$ for all $k = 1, \dots, n$ where d_T is the threshold specified by equation (5). Otherwise this adapted RAIM algorithm decides that an incorrect measurement exists.

Fault Identification Method

If an incorrect measurement is detected by the fault detection algorithm, then the fault identification algorithm also uses the matrices \mathbf{P}_k for the identification of this incorrect measurement. The removal of the first row of a matrix \mathbf{P}_k yields the $(n-m-1) \times n$ matrix \mathbf{L}_k . Furthermore, an orthogonal $(n-m-1) \times (n-m-1)$ matrix $\mathbf{F}_{k,q}$ is chosen so that the first element of the q th column of the $(n-m-1) \times n$ matrix $\mathbf{Z}_{k,q} = \mathbf{F}_{k,q} \mathbf{L}_k$ is equal to $z_{1q}^{(k)}$ and all other elements of the q th column of $\mathbf{Z}_{k,q}$ are equal to zero except for the k th column of $\mathbf{Z}_{k,q}$ (i.e. $q \in N \wedge q \neq k$ with $N = \{1, \dots, n\}$). If $\mathbf{z}_{k,q}^T$ ($k = 1, \dots, n; q = 1, \dots, k-1, k+1, \dots, n$) are the first rows of the matrices $\mathbf{Z}_{k,q}$, then the identification values are given as follows:

$$h_{k,q} = \mathbf{z}_{k,q}^T \mathbf{y} \quad (12)$$

The threshold d_T , which is specified by equation (5), is used by this fault identification algorithm, too. If no subscript j , which fulfils the condition

$$|h_{k,j}| > d_T \forall k \in \{k \in N | k \neq j\} \wedge |h_{j,q}| \leq d_T \forall q \in \{q \in N | q \neq j\}, \quad (13)$$

exists with $j \in N$, then this fault identification algorithm is not available. Otherwise this condition is fulfilled by a subscript j and this fault identification algorithm is available. The measurement, which belongs to this unique subscript j , is identified by this fault identification algorithm as the incorrect measurement in this case.

GIC CONTRIBUTION TO USER INTEGRITY MONITORING

The failure sources, which affect the Galileo satellite measurements of a user receiver, are multifarious where the GIC can only monitor a part of these failure sources. For instance, local failure sources, which only corrupt the measurements of the user receivers located close to these local failure sources, as extreme multipath (e.g., due to satellite signal reflections on the surface of an aircraft, i.e. on the surface of the user itself), extreme ionosphere, poor user/satellite geometry (e.g., due to aircraft banking maneuvers), satellite signal interferences and/or jammer signals are not observable by the GIC. Note that the failure sources of the user receivers cannot be monitored by the GIC, too. Therefore, the GIC cannot check the (full) integrity at user level so that the users have in any case to apply RAIM like techniques. This means that the GIC can only verify the (partial) integrity of the ground control and space segments (i.e. ephemeris and clock errors of the satellites). On the other hand, a user receiver can detect at maximum $n-m$ incorrect measurements among the used measurements so that the integrity of the user navigation solution increases, when the user utilizes the integrity information provided by the GIC.

The general purpose of the GIC is the verification of the SISA values, which are provided by Galileo to the users. This SISA verification is performed by checking whether or not the SISA of each individual satellite bounds the corresponding measurement error component, which is caused by the combined ephemeris and clock error of the corresponding satellite, at all user locations, which lie within the Galileo service area, with a specified probability P_{SISA} , which is either derived from the user performance requirements or an appropriate value defined by Galileo. This means that the ground-based integrity monitoring only checks whether or not the condition

$$P_{SISA} \leq P(|X_k| < SISA_k) = F_k(SISA_k) - F_k(-SISA_k) \quad (14)$$

holds at the worst user location for each individual $SISA_k$. $SISA_k$ denotes the SISA of the k th satellite and $F_k(x_k) = P(X_k < x_k)$ is the actual probability distribution function of the actual measurement error component X_k , which belongs to the k th satellite and which is caused by the combined ephemeris and clock error of the k th satellite, at the worst user location for $SISA_k$.

The current Galileo baseline specifies the subdivision of the world into seven regions and the provision of global integrity (CAS1 and GAS service) and regional integrity (SAS service). It also defines the transmission of one global SISA for each satellite and a corresponding regional integrity flag. Each of these regional integrity flags shall consist of two bits with the information "Not

GALILEO HYBRIDISATION WITH OTHER NAVIGATION SYSTEMS AND/OR SENSORS

Monitored”, “Don't Use” or “Usable”. If a Galileo satellite can not be monitored by the ground-based integrity monitor of a region (e.g., due to insufficient measurements), then the corresponding integrity flag is set to “Not Monitored”. If the satellite can be monitored and the SISA of this satellite bounds the corresponding measurement error component, which is caused by the combined ephemeris and clock error of this satellite, at all user locations, which lie within this region, with the specified probability P_{SISA} , then the integrity flag is set to “Usable”. Otherwise, if the SISA is not bounded, then the corresponding integrity flag is set to “Don't Use”.

It is assumed that only satellite failures affect the measurements of a user receiver as well as that each satellite failure results in a position solution error, which exceeds the alarm limit of this user receiver with a probability, that is equal to one. Assuming further that the probabilities of available and within the specified accuracy operating integrity monitoring functions (i.e. GIC and user integrity monitor) are also equal to one, then the probability of at least one undetected satellite failure (integrity risk) with respect to a user receiver and the probability of loss-of-function (continuity risk) regarding this user receiver are given as follows:

$$P_{uf} = 1 - (1 - P_F \cdot P_{md,G} \cdot P_{md,U})^n \quad (15)$$

$$P_{uf} \approx n \cdot P_F \cdot P_{md,G} \cdot P_{md,U}$$

$$P_{lof} = P_{fa,U} + (1 - P_{fa,U}) \sum_{i=n-m+1}^n \binom{n}{i} P_{fa,G}^i (1 - P_{fa,G})^{n-i} \quad (16)$$

$$P_{lof} \approx P_{fa,U}$$

where

P_{uf}	Probability of at least one undetected failure satellite (i.e. integrity risk) at user
P_F	Probability of a Galileo satellite failure
$P_{md,G}$	Conditional probability of missed detection for the GIC on the condition that a Galileo satellite has failed
$P_{md,U}$	Conditional probability of missed detection for the user on the condition that a Galileo satellite has failed and that this faulty satellite has not been detected by the GIC
P_{lof}	Probability of loss-of-function (i.e. continuity risk) at user
$P_{fa,U}$	Probability of false alarm for the user
$P_{fa,G}$	Probability of false alarm for the GIC
n	Number of user measurements
m	Number of unknowns at user

It must be noted that P_F is the reliability figure (failure probability) of Galileo.

The addition of measurements from further navigation systems and/or from other sensors to the Galileo satellite measurements generally increases the user integrity monitoring availability, since the number of available measurements at the user receiver significantly increases. Note that the adapted RAIM algorithm, which was briefly described above and which is obtained by the modification of the RAIM method proposed by Brenner [1], can also be used by a user integrity monitor when Galileo is hybridised with other navigation systems (e.g. GPS, LORAN-C) and/or with further sensors (e.g. INS, barometer).

If a user receiver uses measurements from further navigation systems as GPS and/or LORAN-C in addition to the Galileo satellite measurements, then the unknowns are the three user receiver position coordinates and the user receiver clock offsets with respect to the Galileo network time as well as to the network times of these other navigation systems. Thus, the first three components of the $m \times 1$ vector \mathbf{x} , which is specified by equations (1) and (4), are the three components of the user receiver position deviation from the predicted user receiver position and the remaining components of this vector \mathbf{x} are the user receiver clock offset deviations from the predicted user receiver clock offsets. For instance, the number of unknowns is equal to five and the design matrix \mathbf{G}_M , which is defined by equation (1), is of the form

$$\mathbf{G}_M = \begin{bmatrix} \bar{g}_{1,1} & \bar{g}_{1,2} & \bar{g}_{1,3} & 1 & 0 \\ \vdots & \vdots & \vdots & \vdots & \vdots \\ \bar{g}_{n_1,1} & \bar{g}_{n_1,2} & \bar{g}_{n_1,3} & 1 & 0 \\ \tilde{g}_{n_1+1,1} & \tilde{g}_{n_1+1,2} & \tilde{g}_{n_1+1,3} & 0 & 1 \\ \vdots & \vdots & \vdots & \vdots & \vdots \\ \tilde{g}_{n_1+n_2,1} & \tilde{g}_{n_1+n_2,2} & \tilde{g}_{n_1+n_2,3} & 0 & 1 \end{bmatrix} \quad (17)$$

when Galileo is only hybridised with GPS and when the number of Galileo satellite measurements is equal to n_1 with $n_1 > 0$ as well as when the number of GPS satellite measurements is equal to n_2 with $n_2 = n - n_1 > 0$. The first three elements $\bar{g}_{i,j}$ ($i = 1, \dots, n_1; j = 1, 2, 3$) of the i th row of \mathbf{G}_M are the components of the 3×1 unit vector pointing from the corresponding Galileo satellite position to the predicted user receiver position and the first three elements $\tilde{g}_{k,j}$ ($k = n_1+1, \dots, n_1+n_2; j = 1, 2, 3$) of the k th row of \mathbf{G}_M are the components of the 3×1 unit vector pointing from the corresponding GPS satellite position to the predicted user receiver position in this case.

On the other hand, if Galileo is hybridised with a barometric altimeter, then only one additional measurement is available at the user receiver. The third element of the row, which belongs to this barometric altimeter measurement, of the design matrix specified by equation (1) is equal to one and all other elements of this row are equal to zero in this case. Moreover, the unknowns are the three user receiver position coordinates and the user receiver clock offset with respect to the Galileo network time (i.e. the number of unknowns is equal to four) when Galileo is only hybridised with a barometer.

RLS Approach for RAIM/INS Hybridisation

In the following, an approach for the hybridisation of a Galileo receiver with an Inertial Navigation System (INS) by means of a Recursive Least Squares (RLS) algorithm is given. Since many RAIM algorithms currently in use are based on least squares adjustment (see RAIM algorithm presented above), the envisaged RLS approach offers a simplified way for RAIM augmentation to inertial sensors. In order to include the INS dynamics, a state vector augmentation is necessary as well as the incorporation of the INS characteristics using covariance propagation. This approach enables an easy transition from a snapshot algorithm to a recursive algorithm, which preserves the history information.

To see the transition from the LS to RLS algorithm more clearly, the least squares adjustment equations shall be demonstrated shortly. Denoting H as observation matrix and y as measurement residuals vector, the best estimate of the unknowns x (three positions and time offset) can be given as:

$$\hat{x}_{LS} = (H^T H)^{-1} H^T \cdot y \quad (18)$$

The equation from which the measurement residuals estimate can be calculated is

$$\hat{y} = H \hat{x}_{LS} \quad (19)$$

Performing the transition from a snapshot based algorithm as shown above to a sequential algorithm results in the following (unweighted) Recursive Least Squares adjustment, which can be found in literature:

$$x_k = \Phi_{k-1} \cdot x_{k-1} + w_{k-1} \quad (20)$$

$$y_k = H_k \cdot x_k + v_k \quad (21)$$

$$\hat{x}_k = (H_k^T H_k + \tilde{\Lambda}_k)^{-1} \cdot (\tilde{\Lambda}_k \tilde{x}_k + H_k^T y_k) \quad (22)$$

with

$$\hat{\Lambda}_k = H_k^T H_k + \tilde{\Lambda}_k \quad (23)$$

and

$$\tilde{P}_k = \Phi_{k-1} \hat{P}_{k-1} \Phi_{k-1}^T + Q_{k-1} \quad (24)$$

Note, that the matrix $\tilde{\Lambda}_k$ is commonly referred to as the information matrix, $\hat{P}_k = \hat{\Lambda}_k^{-1}$ is the estimation of the covariance matrix of the state vector error estimate and $\tilde{P}_k = \tilde{\Lambda}_k^{-1}$ is the concerning predicted covariance matrix. Thus INS characteristics can be incorporated using the covariance propagation in \hat{P}_k , respectively $\hat{\Lambda}_k^{-1}$, by means of the transition matrix Φ_k . Note further that for covariance propagation calculations, only equations (23), (24) and the inversions $\hat{P}_k = \hat{\Lambda}_k^{-1}$ as well as $\tilde{P}_k = \tilde{\Lambda}_k^{-1}$ are relevant. The terms v_k and w_k denote measurement noise and process noise and Q_k is the (diagonal) covariance matrix of w_k . In the special case when the LS estimate is to be weighted, then a weighting Matrix W has to be included in $\hat{\Lambda}_k$ as follows:

$$\hat{\Lambda}_k = H_k^T W H_k + \tilde{\Lambda}_k \quad (25)$$

Note, that $\hat{\Lambda}_k$ increases (disregarding the time dependency) as the standard deviations contained in W decreases, just as the information that can be surmised from a measurement increases as the noise decreases. $\hat{\Lambda}_k$ does not depend on actual data, but on the statistics of the process noise and the matrix H that relates the vector x to the noisy measurements.

In order to cope with the dynamical behaviour of an inertial navigation system, the main characteristics of an INS (albeit here some simplifications are made) have to be incorporated into the equations given above. In contrast to a satellite navigation system or a barometric sensor, which have (more or less) uncorrelated outputs with respect to time, an INS has a history dependent output, i.e. the position determination process is performed by a double integration of the accelerometers output. The dynamics of the INS have been taken into account by using the transition matrix Φ_k . In the simplest case, the model used in the transition matrix for the prediction of the state vector from one epoch to the other has to include a velocity dependency. Thus, also a state vector augmentation to include the INS dynamics is necessary, leading to the following equation:

$$\begin{pmatrix} x_k \\ \dot{x}_k \\ dT_k \end{pmatrix} = \begin{bmatrix} I & \Delta & 0 \\ 0 & I & 0 \\ 0 & 0 & 1 \end{bmatrix} \cdot \begin{pmatrix} x_{k-1} \\ \dot{x}_{k-1} \\ dT_{k-1} \end{pmatrix} + w_{k-1} \quad (26)$$

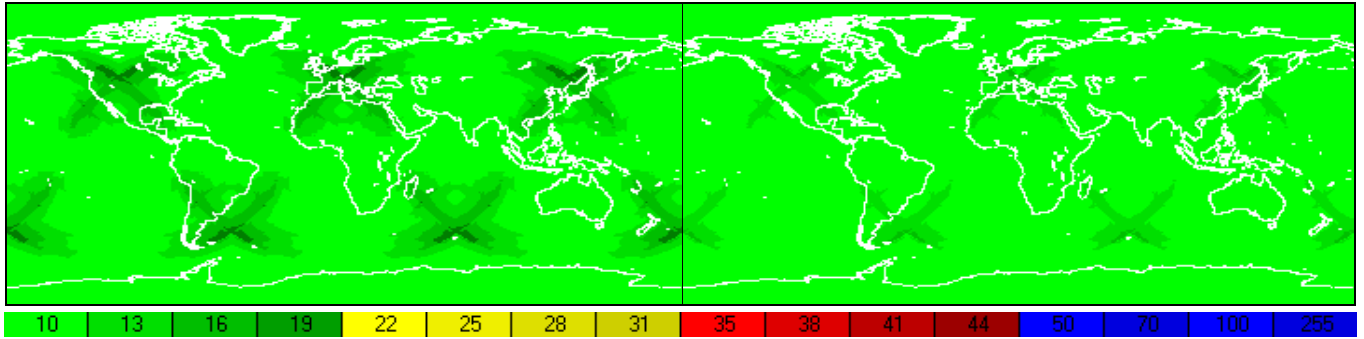


Figure 1. Horizontal Protection Level [m] for Galileo at 9th of June 2000, 01:00:00 (Left: Worst Case; Right: Good Case)

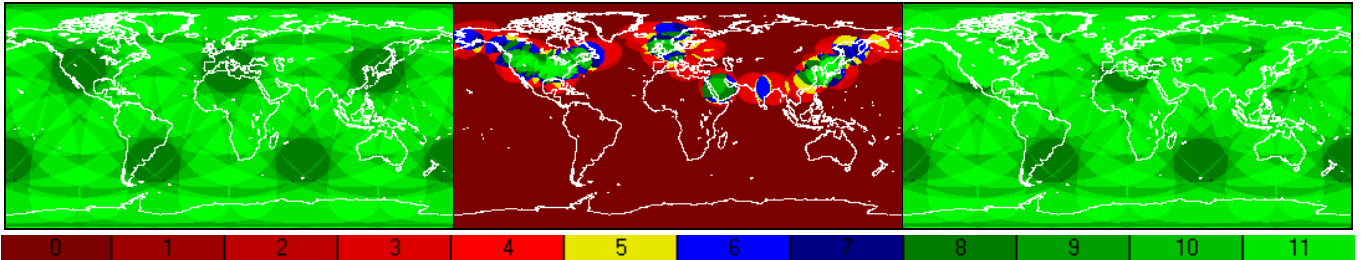


Figure 2. Galileo/LORAN-C Visibility at 9/62000, 01:00:00 (Left: Galileo; Center: LORAN-C Stations; Right: Combined Galileo Satellite and LORAN-C Station Visibility)

where now x does not only contain the 3 positions and time offset dT_k , but also 3 velocity components w.r.t. the sampling interval Δt . I denotes the 3x3 identity matrix and Δ denotes the 3x3 diagonal matrix with Δt as diagonal elements. A more sophisticated transition model may use a navigational error model for a free inertial system.

ADAPTED RAIM ALGORITHM AVAILABILITY SIMULATION

A first preliminary qualitative assessment of the integrity monitoring level, which can be achieved at user level, was performed by means of an availability simulation using the adapted RAIM algorithm described above.

Simulation Assumptions

Table 1 shows the Galileo constellation parameters used for the adapted RAIM algorithm availability simulation.

Table 1. Galileo Satellite Constellation Parameters [2]

Parameter	Simulation Assumption
Walker Constellation	30/3/0
Altitude	23322.371 km
Inclination	54°
Eccentricity	0

The Optimized 24 GPS Constellation, specified in document RTCA/DO-229B [6] was used for this simulation. A common ephemeris reference epoch for Galileo and GPS was used and set to the 4th of June 2000 (2000, 6, 4,

00:00:00) for the availability simulation. In addition to this, the LORAN-C stations specified by the Loran-C Chain Information document [4] were used for this simulation. Furthermore, the simulation was performed world-wide for the 9th of June 2000 over 24 hours with a sampling time of 600 s as well as with a grid spacing of 1°. The CAT I user performance requirements, for the simulation are shown in the following table.

Table 2. CAT I User Performance Requirements [3]

Parameter	Simulation Assumption
Continuity Risk	10^{-5} per Approach
Integrity Risk	$4 \cdot 10^{-8}$ per Approach
Vertical Alarm Limit (VAL)	10 m
Time To Alarm (TTA)	6 s

It was additionally assumed that HAL=10m, elevation mask angle=5°, correlation time t_{CT} =360s, $\sigma_{GPS, no SA}$ =8m, σ_{Baro} =50m, $\sigma_{Loran-C, nominal}$ =61.5m and $\sigma_{Loran-C, accurate}$ =4 m. Moreover, an elevation dependent standard deviation (1.1 m - 4.3 m) of Galileo measurement errors was used, that CAT I approach period=150s and it was assumed that only one user, which conducts a CAT I approach, is affected by a satellite failure, which is not detected by the GIC, at a time. Therefore, the CAT I continuity risk rate r_{CR} , which is equal to $6.67 \cdot 10^{-8}/s$, and the CAT I integrity risk rate r_{IR} , which is equal to $2.67 \cdot 10^{-10}/s$, were used for the availability simulation so that the probability of at least one undetected satellite failure (P_{uf}) regarding a user receiver is given by $P_{uf} = r_{IR} \cdot t_{CT} = 9.6 \cdot 10^{-8}$ and the probability of loss-of-function (P_{lof}) with respect to this user receiver is

determined by $P_{lof} = r_{CR} \cdot t_{CT} = 2.4 \cdot 10^{-5}$. A visibility simulation for the used Galileo satellite constellation, for the used LORAN-C stations and for the hybridisation of Galileo with LORAN-C showed that the number of visible Galileo satellites is, on average, equal to 10 at user level, i.e. $n = 10$ for Galileo (see Figure 2). Thus, the adapted RAIM algorithm availability simulation was performed for the following two cases where it was also taken into account that $P_{md,U}$ (i.e. the conditional probability of missed detection for the user on the condition that a Galileo satellite has failed and that this faulty satellite has not been detected by the GIC) is determined by equation (15).

- (i) **Worst Case (WC):** $P_F = 10^{-1}$, $P_{md,G} = 1$ (i.e. low Galileo reliability, no ground-based integrity monitoring by the GIC) $\Rightarrow P_{md,U} = 9.6 \cdot 10^{-8}$
- (ii) **Good Case (GC):** $P_F = 10^{-4}$, $P_{md,G} = 9.6 \cdot 10^{-2}$ (i.e. higher Galileo reliability, ground-based integrity monitoring by the GIC) $\Rightarrow P_{md,U} = 10^{-3}$

Simulation Results

The following figures show HPL, VPL as well as the adapted RAIM algorithm availability with respect to horizontal/vertical navigation at the grid points of a world-wide grid for the worst case and for the good case where it is also considered that a user receiver uses either only Galileo measurements or combined with GPS, LORAN-C and/or barometric altimeter as well as a simplified INS.

CONCLUSIONS

The current Galileo baseline satellite constellation causes two stripes (world-wide) of poor user integrity monitoring availability with respect to horizontal navigation due to six dynamic areas with “degraded” Galileo satellite visibility, i.e. with only 8 visible Galileo satellites, at user level (see Figure 2 and Figure 4). Moreover, the figures below also show that CAT I user performance requirements, in particular for vertical navigation, cannot be met world-wide and all the time.

If the GIC contributes to the check of the (partial) integrity of the ground control and space segments by performing ground-based integrity monitoring, then the user integrity monitoring availability regarding horizontal navigation increases as can be seen from Figure 4.

Furthermore, a Galileo/GPS combination enhances user integrity availability with respect to horizontal navigation too (see Figure 4 and Figure 7).

Galileo hybridised with LORAN-C and barometer only significantly increases the user integrity availability wrt horizontal navigation when a user receiver uses accurate LORAN-C measurements, i.e. when $\sigma_{LORAN-C} = 4$ m as can be seen from Figure 4, Figure 8 and Figure 9.

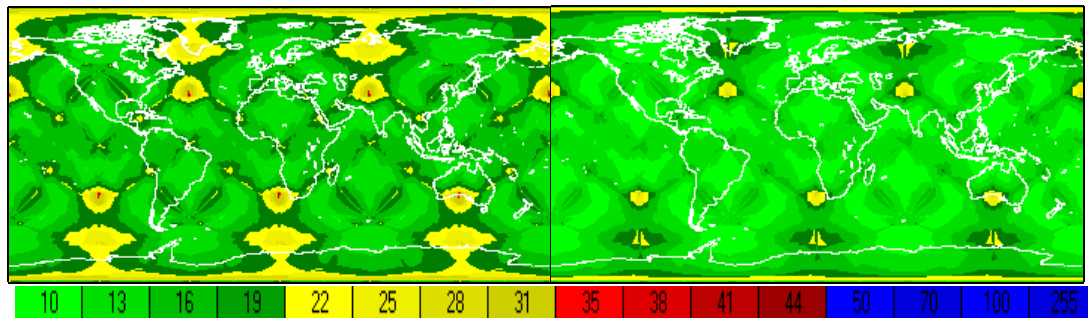


Figure 3. Vertical Protection Level [m] for Galileo at 9/6/2000, 01:00:00 (Left: Worst Case WC; Right: Good Case GC)

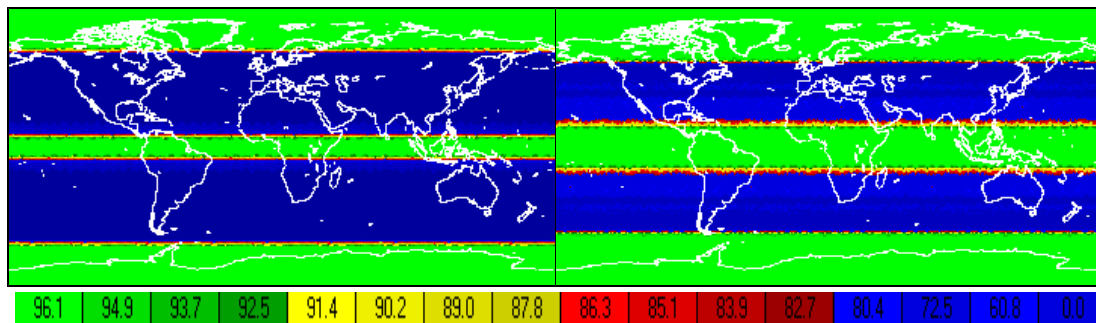


Figure 4. Adapted RAIM Algorithm Availability [%] for Galileo regarding Horizontal Navigation (Left: WC; Right: GC)

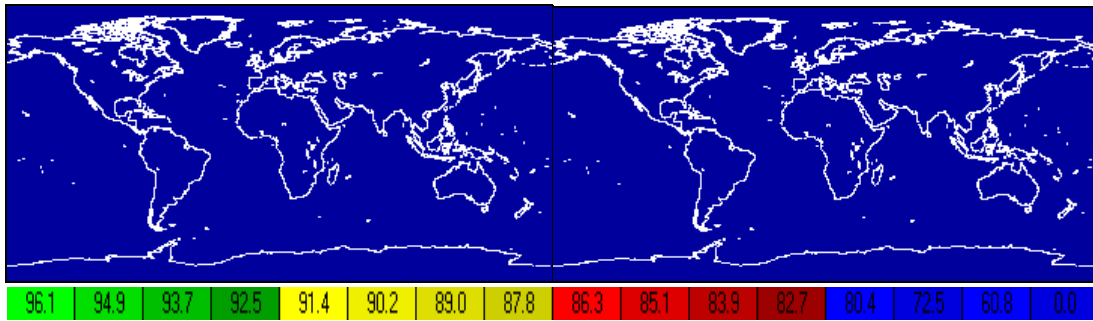


Figure 5. Adapted RAIM Algorithm Availability [%] for Galileo regarding Vertical Navigation (Left: WC; Right: GC)

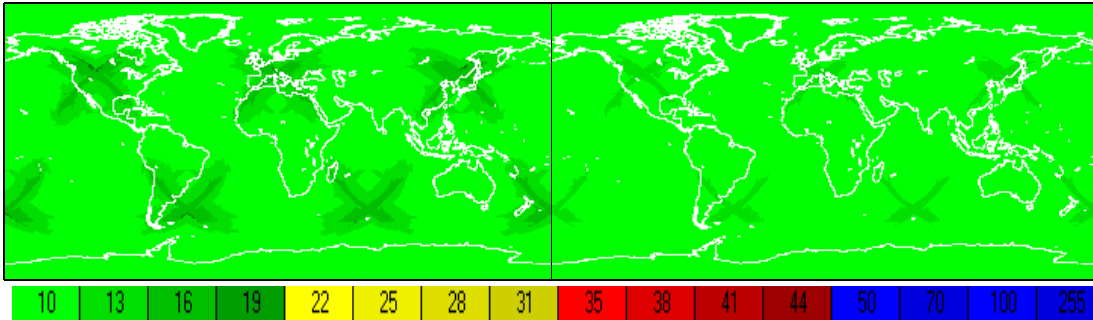


Figure 6. Horizontal Protection Level [m] for Galileo hybridised with GPS at 9/6/2000, 01:00:00 (Left: WC; Right: GC)

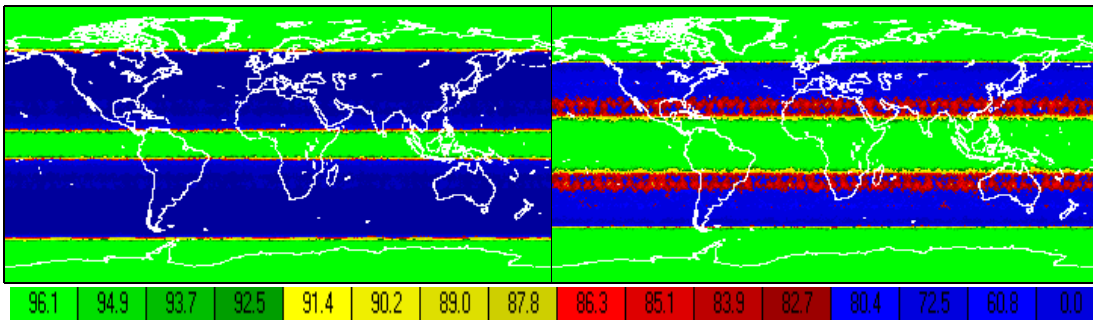


Figure 7. Adapted RAIM Algorithm Availability [%] for Galileo/GPS regarding Horizontal Navigation (Left: WC; Right: GC)

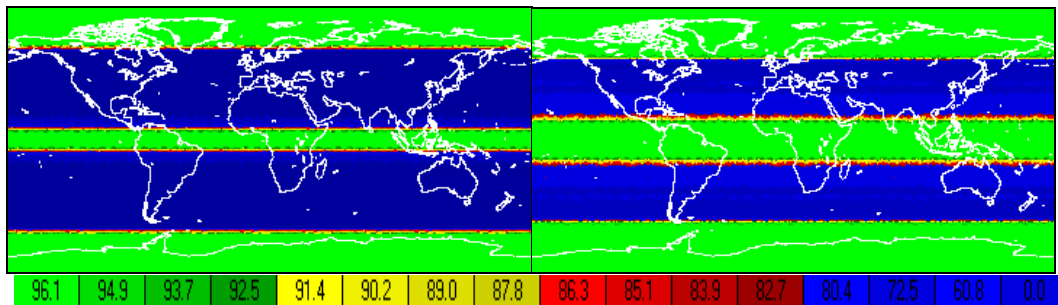


Figure 8. Adapted RAIM Algorithm Availability [%] for Galileo hybridised with LORAN-C and with Barometric Altimeter regarding Horizontal Navigation ($\sigma_{\text{LORAN-C}} = 61.5$ m; Left: Worst Case; Right: Good Case)

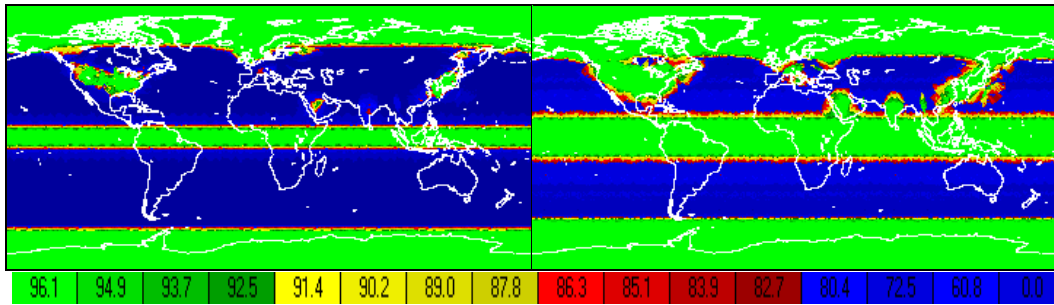


Figure 9. Adapted RAIM Algorithm Availability [%] for Galileo hybridised with LORAN-C and with Barometric Altimeter regarding Horizontal Navigation ($\sigma_{\text{LORAN-C}} = 4 \text{ m}$; Left: Worst Case; Right: Good Case)

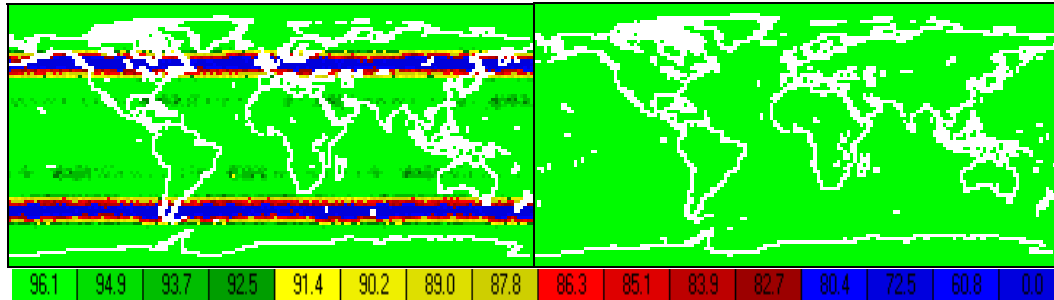


Figure 10. Adapted RAIM Algorithm Availability [%] for Galileo/INS regarding Horizontal Navigation (Left: WC; Right: GC)

Simulation results for the simplified INS approach show improvement capabilities for horizontal RAIM availability (see Figure 4 and Figure 10).

ACKNOWLEDGMENTS

The contributions of the University FAF Munich to this paper have been funded by Deutsches Zentrum für Luft- und Raumfahrt e.V. (DLR) within the Contract No. FKZ:50 NA 9912.

REFERENCES

- [1] Brenner, M., *Implementation of a RAIM Monitor in a GPS Receiver and an Integrated GPS/IRS*, Proceedings of The Third International Technical Meeting of The Satellite Division of The Institute of Navigation, ION GPS-90, Colorado Springs, CO, September 19-21, 1990, pp. 397-406
- [2] *Galileo Overall Architecture Definition Study (GALA): Performance Budget File*, Doc. Ref. No. GALA-ASPI-DD036, Issue 2.0, 20 July 2000
- [3] *Global Navigation Satellite System Panel (GNSSP): Local Area Augmentation of GPS for the Precision Approach of Aircraft*, GNSSP/WG-D/WP-113, Working Group A, B, C, D, Meeting, Presented by Jeff Williams, Gold Coast, Australia, February 17-28, 1997
- [4] *LORAN: Loran-C Chain Information in WGS 84 Coordinates*, <http://www.megapulse.com/table.html>, Megapulse, Inc., N. Billerica, MA, 1999
- [5] *Minimum Operational Performance Standards For Global Positioning System/Wide Area Augmentation System Airborne Equipment*, RTCA Document No. RTCA/DO-229, Prepared by RTCA Special Committee 159 (RTCA SC-159), RTCA, Inc., Washington, D.C., January 16, 1996
- [6] *Minimum Operational Performance Standards For Global Positioning System/Wide Area Augmentation System Airborne Equipment*, RTCA Document No. RTCA/DO-229B, Prepared by RTCA Special Committee 159 (RTCA SC-159), RTCA, Inc., Washington, D.C., October 6, 1999